Direct Theoretical Approach to Jet Propulsion Principles based on Pressure Variation inside the Engine

Himani Sinhmar[1], Pallavi Rastogi[2], Shripad P. Mahulikar[†,3]

[1]Undergraduate Research Student, [2]Research Scholar, [3]Professor

[1-3]Department of Aerospace Engineering, Indian Institute of Technology Bombay, Powai, Mumbai 400076, India.

[1]*E-mail*: himani_sinhmar@iitb.ac.in, [2]*E-mail*: <pallavirastogi@aero.iitb.ac.in>

[†,3]Corresponding Author: spm@aero.iitb.ac.in, Tel. +91-22-25767122

ABSTRACT

This investigation directly explores the first principles of jet propulsion by estimating the pressure forces acting on a simplified turbojet engine model. In a turbojet engine thrust is generated by pressure forces exerted by the fluid on its boundaries and components. Theoretically, thrust and propulsive efficiency are sufficient for understanding the evolution of variety of aircraft engines. A new definition for the propulsive efficiency from the point of view of generated pressure profile utilization by the jet engine is proposed. A simplified model for turbojet engine integrating aerothermodynamics of engine components is developed which exhibits that an engine which can make maximum possible use of fluid pressure profile for thrust would have the highest possible propulsive efficiency. The analysis carried out on this model indicates that the net thrust and redefined propulsive efficiency depend on the engine geometry, inlet velocity and combustion exit temperature of the engine. This study leads to a conclusion that the generation of thrust by the jet engine is due to an increase in the exit area of the turbojet model. Two models of combustor, isobaric combustion and variable pressure combustion

are discussed in detail. These models can be extended to ramjet and scramjet engines such that efficient use of pressure profile is made to achieve higher values of net thrust.

Keywords: Jet Propulsion, Propulsive efficiency, Thrust , Pressure profile of turbojet, Turbojet engine, Variable pressure combustor, Isobaric combustor

NOMENCLATURE

A	: Flow track Area [m^2]
dA	: Elemental Flow track Area [m^2]
d*s*	: Elemental Surface Area [m^2]
F	: Thrust [N]
r	: radius [m]
P	: Pressure (static) [N/m^2]
P_o	: Total Pressure [N/m^2]
T_o	: Total Temperature [N/m^2]
M	: Mach number [-]
T	: Temperature [K]
$T\_$	: Temperature just after a station [K]
v	: Velocity [m/s]
$v\_$	: Velocity just after a station [m/s]
$M\_$	: Mach number just after a station [-]

GREEK SCRIPTS

β : Angle between the outward normal of a surface and the direction of thrust [degrees or radians]

η : Efficiency [-].

π : Ratio of circumference to the diameter of a circle [-].

ρ : Density [kg/m^3].

ρ_- : Density just after a station [kg/m^3].

SUBSCRIPTS

1 : Station 1

2 : Station 2

2′ : Station 2′

3 : Station 3

1-2 : Region between stations 1 and 2

2′-3 : Region between stations 2′ and 3

p : propulsive

∞ : ambient condition

1. Introduction

The approach to the analysis of the mechanics of jet propulsion is largely based on the changes to the parameters of the fluid which interacts with the engine. In the literature various methods to analyze the performance of the aircraft are studied extensively. The basic concept of propulsive efficiency can serve as a powerful analytical tool. J.H. Lewis III [1] approaches propulsive efficiency from the point of view of energy utilization by applying basic thermodynamic principles. This definition accounts for the energy unavailability production into two parts : 1) the unavailable energy associated with the thermodynamic cycle's rejected heat; and 2) the wasted energy produced by inefficiencies inherent to the conversion of available cycle energy to propulsive power. He defines propulsive efficiency as the ratio of actual propulsive power and maximum available propulsive power. The difference between actual and maximum propulsive power is manifested as waste energy which, by virtue of energy conservation, appears in the engine exhaust stream either as residual kinetic energy or as thermal energy. Onder Turan et al. [2-4] studied the exergetic effects of various design parameters on turbojet engine. Exergy is a useful tool in marking out the limits of maximum work for cycle efficiency. It is the work that could be obtained by a system in a reversible process from a given state to a state of equilibrium with the environment. He found that any increase in compressor pressure ratio along with increase in flight Mach number results in an increasing exergy efficiency of the engine. However, increasing turbine inlet temperature decreases the exergy efficiency of the small turbojet engine. Pedro Patrico and Jose M. Tavares [5] discusses the behavior of ideal jet engine and present simple analytical expressions for overall efficiency and reduced thrust. These performance measures are shown to depend on the ratio of the temperature at the turbine to the inlet temperature (T_3/T_i). An analysis of these expressions then show that it is not possible to choose an optimal set of values of compression ratio and T_3/T_i that maximizes both the overall efficiency and thrust.

These studies report the performance parameters of turbojet by analyzing the effect of fluid on jet engine. But there are no reported studies that theoretically investigate the effect of pressure variation inside the jet engine or equally, the engine geometry on the performance parameters of a turbojet. Thrust produced by a jet engine is given by the product of fluid mass flow rate entering the engine and the velocity change of the fluid on passing through the engine plus the pressure thrust (in case of incomplete expansion) [6]. Though this expression gives the force that the jet engine exerts on the fluid, by Newton's third law this is same as the force acting on the jet engine. To calculate the thrust produced by the jet engine without using Newton's law would mean finding the pressure force exerted by the fluid on the boundaries and the components of the jet engine [7]. This proposition at first thought seems unfriendly due to the complex geometry of the internal components of the jet engine. Also the relationships available for the performance parameters based on the fluid velocity are simple algebraic expressions. Nevertheless this direct approach establishes unity amidst its diverse manifestations. It also takes care of the complications which have prevented the tackling of the jet engine by means of the pressure variations inside the engine. Thrust and propulsive efficiency are sufficient for the philosophical understanding of the generation of variety of aircraft engines. The wide spread of jet engines, ranging from rocket engine, scramjet and ramjet engine, turbojet engine, turbofan engine (mixed and unmixed exhausts), to turboprop engine, can be clearly explained based on this direct approach.

A fluid exerts pressure normal to the surface over which it flows. In a jet engine, the resultant of the fluid pressure forces in the direction of motion is thrust. Hence for a surface whose outward normal subtends an angle in the first or fourth quadrant with the direction of motion will give positive thrust and that which subtends an angle in the second or third quadrant will give negative thrust. Therefore, a convergent nozzle will give negative thrust. Negative thrust may be viewed as a necessary evil to maintain the positive thrust which cannot be maintained by only combustion temperature due to limitation on its maximum value. An engine which can make maximum possible use of the fluid pressure profile for thrust would have the highest possible propulsive efficiency.

1.1 Objectives and scope

The objective of this theoretical research is to evaluate the effects of design and thermodynamic parameters on the propulsive performance of a turbojet engine by analyzing the pressure profile developed by the engine. It presents a methodology to generate the seemingly complex pressure profile of an engine with the aid of a simplified turbojet model, which can be easily extended to other varieties of aircraft such as turbofans, ramjets and scramjets. Conventional propulsive efficiency is based on the rate of energy utilization but the aim of this study is to relate propulsive efficiency to the maximum utilization of the engine pressure profile. Now a days there is an increased emphasis on efficient use of fuel energy, this direct approach can provide essential insight to help the aircraft performance analyst in improving the engine design and analysis process. This investigation leads to a relation between the generation of thrust by the jet engine and the ratio of the inlet and exit area of the turbojet.

Modeling of jet engine would differ based on the type of heat addition taking place in the combustor (assuming isentropic compression and expansion in the inlet-compressor and the turbine-nozzle region). Heat addition can take place either via constant pressure combustion in a variable area duct or via variable pressure combustion in constant area duct. Both the models will be discussed here.

2 Theoretical Model of Jet Engine

Fig. 1 shows the theoretical model of jet engine with variable pressure combustor. Station 1 is the inlet and 3 is the exit. Station 2 to 2′ represents the combustion chamber. The direction of motion of fluid flow is represented by axis z. The area of the jet engine varies with distance z. At the same time it is assumed that all the flow properties are uniform across any given cross section of the flow and hence are functions of z only. Such a flow, where A = A(z), P = P(z), $\boldsymbol{\rho} = \boldsymbol{\rho}(z)$ and $\mathbf{v} = \mathbf{v}(z)$ for steady flow is defined as quasi-one dimensional flow. It is this *area change* that causes the flow properties to vary as a function of z [6]. In the model presented it is assumed that the flow is steady, inviscid and quasi 1 dimensional. Further, the gas is assumed to be calorically perfect and that the contribution of the fuel mass flow rate to the gas in the duct is small. Hence, combustion is modeled as heat transfer through the wall. The meridian shape of the jet engine is irrelevant with the 1D isentropic model and the flow is only dependent on cross section area ratios [9]. Therefore, final thermodynamic parameters from station 1 to 2 or station 2′ to 3 do not depend on nature of the radius variation but only on the local value of the radius.

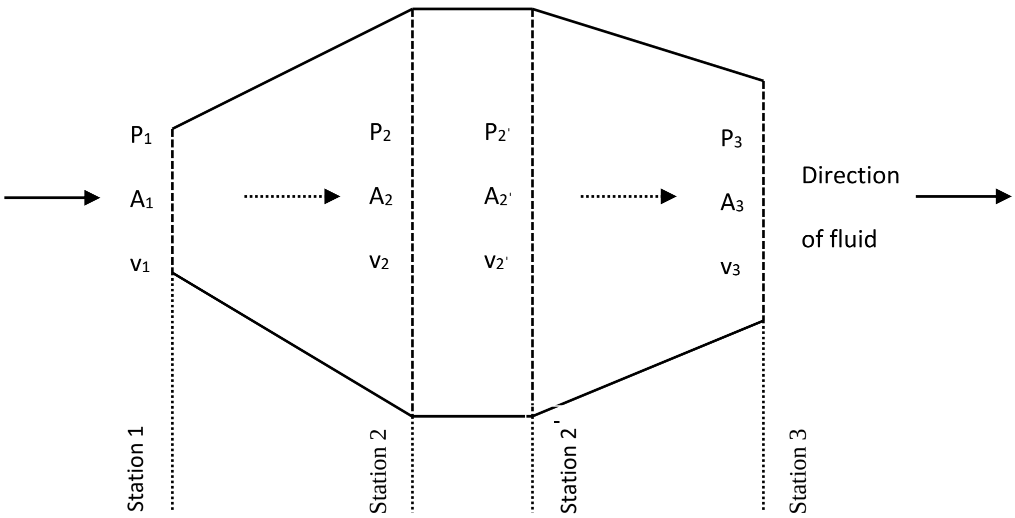

Fig.1 Theoretical model of turbojet engine for variable pressure combustion

2.1 Variable pressure combustion in constant area duct

Due to heat addition there is an increase in the temperature from T_2 to T_2' and a decrease in the pressure from P_2 to P_2' which results in reduction of density from ρ_2 to ρ_2'. This can be explained based on the *Rayleigh curve* [6]. As the flow is subsonic at the entrance of the combustion chamber, heat addition leads to an increase in Mach number, decrease in pressure and an increase in velocity. For optimal expansion, the pressure at station 3 is P_1 (same as that at station 1). All the dynamic head is provided by the compressor in a practical jet engine and the ram flow is provided by means of the velocity v_1 at station 1. This does not include the dynamic head needed to run the compressor. The flow passage from station 1 to 2 corresponds to the subsonic diffusion in the intake and the compressor. In a practical compressor, in addition to the stator, diffusion also occurs in the rotor and the amount of diffusion in the rotor is indicated by the degree of reaction of the stage. Hence the region from station

1 to 2 represents the intake and the compressor in a practical jet engine and the region from station 2′ to 3 represents the turbine and the nozzle. As shown in Fig. 1, from station 1 to 2 the flow track area keeps increasing whereas in an axial flow compressor the flow track area keeps reducing since dynamic head is polytropically added to the flow. A similar argument can be put forth to explain the decreasing flow track area from station 2′ to 3 and increasing flow track area in an axial flow turbine.

2.1.1. Thrust provided by the jet engine

A high compressor pressure ratio is desirable as thermodynamics claims that the basic cycle efficiency increases with pressure ratio and higher operating temperature enables higher amount of work to be obtained from the thermodynamics cycle [7,8]. This is also reflected in the mathematical definition for thrust

$$F = \int (P - P_\infty) cos\beta ds \qquad \text{Eq. (2.1)}$$

where the integral has to be performed over the entire surface of the jet engine and its components.

2.1.2 Approach developed to compute thrust

In the case of optimal expansion, the pressure increases from P_1 to P_2 in the diffuser region from station 1 to 2 and drops back to P_1 at station 3. β is the angle subtended by the outward normal with the direction of motion of the aircraft.

$$\mathrm{F} = \int_1^2 (\mathrm{P} - \mathrm{P}_\infty).\,cos\beta.\,\mathrm{d}s + \int_{2\prime}^3 (\mathrm{P} - \mathrm{P}_\infty).\,cos\beta.\,\mathrm{d}s \qquad \text{Eq.(2.2)}$$

From station 1 to 2 and station 2′ to 3, β remains constant. Hence Eq. (2.2) may be written as

$$\mathrm{F} = cos\beta_{1\text{-}2}\int_1^2 (\mathrm{P} - \mathrm{P}_\infty).\mathrm{d}s + cos\beta_{2'\text{-}3}\int_{2\prime}^3 (\mathrm{P} - \mathrm{P}_\infty).\mathrm{d}s \qquad \text{Eq.(2.3)}$$

To account for the $cos\beta$.ds term in Eq. (2.2), the pressure may be projected on two annular disks as shown in Fig. 2. The two disks 1 to 2 and 2′ to 3 have outer radii r_2. The inner radius of disk 1 to 2 is

r_1 while that of disc $2'$ to 3 is r_3 , where $r_1 < r_3$. Heating the flow at station 2 reduces the density of fluid in the region $2'$ to 3 and to maintain continuity the flow track area increases, thereby reducing the area projected of disc $2'$ to 3 in Fig. 2. It is because of this reduction in area of disc $2'$ to 3 due to the rise in temperature that generates thrust. If the temperature is not raised at station 2 then A_3 would be equal to A_1 and no thrust would be obtained as is indicated by Eq. (2.4). The mathematical proof for this claim is given in subsection *2.1.6*.

The evaluation of thrust of the jet engine shown in Fig. 1 now reduces to the evaluation of forces acting on the discs 1 to 2 and $2'$ to 3 and subtracting them. Hence Eq. (2.2) can be written as

$$F = \int_{\{Disk\ 1-2\}} (P(r) - P_\infty) dA - \int_{\{Disk\ 2'-3\}} (P(r) - P_\infty) dA \qquad \text{Eq.(2.4)}$$

where P(r) is found by solving the governing equation of fluid flow and dA = 2πrd$r$. Hence Eq. (2.4) reduces to

$$F = \int_{r1}^{r2} (\mathrm{P} - \mathrm{P}_\infty)\, 2\pi r\, dr - \int_{r_{2'}}^{r3} (\mathrm{P} - \mathrm{P}_\infty) 2\pi r\, \mathrm{d}r \qquad \text{Eq.(2.5)}$$

which may be written as

$$\mathrm{F} = 2\pi \left[\int_{r1}^{r2} \{\mathrm{P(r)} - \mathrm{P}_\infty\}\, r\, \mathrm{d}r - \int_{r2'}^{r3} \{\mathrm{P(r)} - \mathrm{P}_\infty\}\, r\, \mathrm{d}r \right] \qquad \text{Eq.(2.6)}$$

2.1.3 Redefining Propulsive Efficiency

It is clear that from station 1 to 2, β takes values in the I and the IV quadrant, keeping $\cos\beta > 0$. Similarly, from station $2'$ to 3, $\cos\beta$ is negative, thereby contributing negatively to the thrust. This is in consistency with the contribution of inlet - compressor and turbine - nozzle to the net thrust in actual jet engine [7]. As the temperature T_2' increases, β in the region $2'$ to 3 decreases (approaching 90°) thereby reducing the negative thrust (Refer section *2.1.6*). Hence if thrust is to increase in addition to increase in P_2', T_2' must increase in order to reduce the negative thrust. In a jet engine negative thrust is always present because T_2' cannot increase indefinitely due to limitations in material cooling technology.

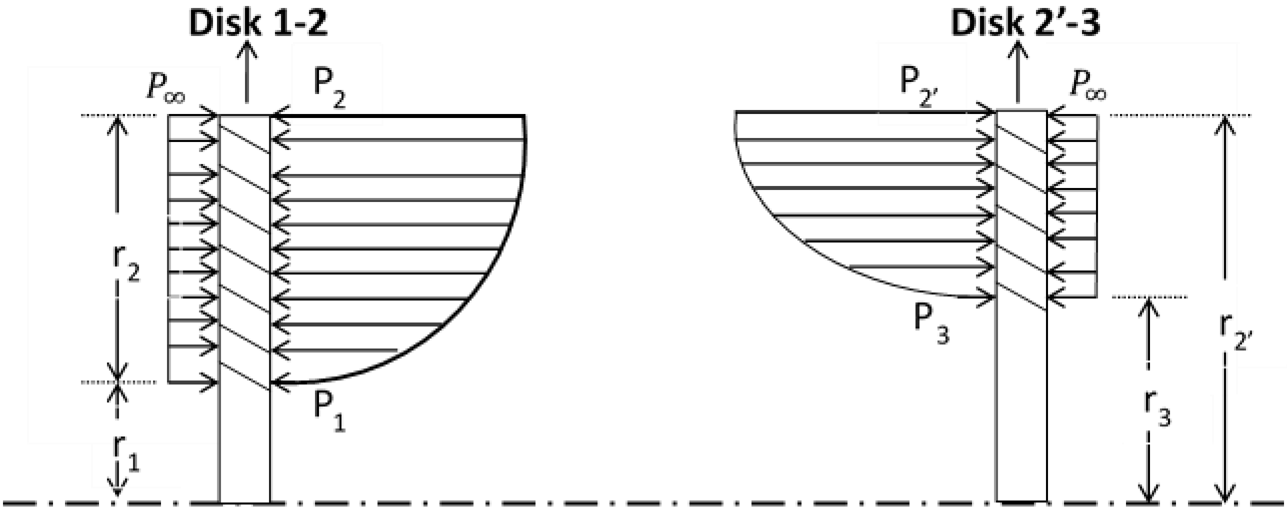

Fig.2 Projection of pressure profile on annular disks

Due to the presence of negative thrust, fluid forces cannot be utilized fully for the generation of net thrust. Therefore, a new definition of the propulsive efficiency is proposed in order to indicate how efficiently fluid pressure forces are utilized for the generation of thrust. It may be mathematically redefined as

$$\eta_p = \frac{\int (\mathrm{P} - \mathrm{P}_\infty)\, cos\beta \,\mathrm{d}s}{\int (\mathrm{P} - \mathrm{P}_\infty)\,\mathrm{d}s} \qquad \text{Eq.(2.7)}$$

2.1.4 Numerical Results

Following analysis is carried out for subsonic inlet flow with optimal expansion in the nozzle. P_1 and T_1 depend on the altitude at which the aircraft is flying and hence are known. Also, M_∞ is different from M_1 as explained in the section 2.1. Thermodynamic parameters at station 2 are solved using conservation equations and equation of state. The pressure variation in region 1 to 2 is obtained using Eq. (2.8).

$$\frac{v_1 \mathrm{A}_1}{\mathrm{A}} = \left(\frac{\mathrm{P}}{\mathrm{P}_1}\right)^{\frac{1}{\gamma}} \sqrt{2\,\mathrm{C_p}\left(\mathrm{T}_{01} - \mathrm{T}_1.\left(\frac{\mathrm{P}}{\mathrm{P}_1}\right)^{\frac{\gamma-1}{\gamma}}\right)} \qquad \text{Eq.(2.8)}$$

Where

$$\mathrm{T}_{01} = \mathrm{T}_1\left(1 + \frac{\gamma - 1}{2}\mathrm{M}_1^2\right) \qquad \text{Eq. (2.8.1)}$$

$$v = \sqrt{2\,\mathrm{C_p}\left(\mathrm{T}_{01} - \mathrm{T}_1\left(\frac{\mathrm{P}}{\mathrm{P}_1}\right)^{\frac{\gamma-1}{\gamma}}\right)} \qquad \text{Eq. (2.8.2)}$$

$$\mathrm{T} = \mathrm{T}_1\left(\frac{\mathrm{P}}{\mathrm{P}_1}\right)^{\frac{\gamma-1}{\gamma}} \qquad \text{Eq. (2.8.3)}$$

From station 1 to 2 and station 2′ to 3 engine is modeled with a constant β. For station 2 to 2′

$$\frac{\mathrm{P}_{2'}}{\mathrm{P}_2} = \frac{1 + \gamma \mathrm{M}_2^2}{1 + \gamma \mathrm{M}_{2'}^2} \qquad \text{Eq. (2.9)}$$

$$\mathrm{M}_{2'} = \mathrm{M}_2 \frac{\mathrm{P}_2}{P_{2'}} \sqrt{\frac{T_{2'}}{\mathrm{T}_2}} \qquad \text{Eq. (2.10)}$$

T_2' is the turbine inlet temperature that is limited by the maximum temperature that turbine blades can sustain. Using Eq. (2.9) and Eq. (2.10), P_2' and M_2' are calculated. It is assumed that the C_p (specific heat at constant pressure) of the fuel-air mixture is same as the C_p of ambient air. For a given M_1, combustion temperature T_2' will vary with A_2/A_1.i.e. the size of the jet engine. This is to satisfy the condition that turbine inlet Mach number (M_2') is always subsonic and the exit Mach number $M_3 \leq 1$. Eq. (2.11) and Eq. (2.12) are used to obtain the range of the T_2' for a given A_2/A_1.

$$\mathrm{M}_{2'} = \frac{\mathrm{T}_{2'} v_2}{\mathrm{T}_2\sqrt{\gamma \mathrm{R} \mathrm{T}_{2'}}} < 1 \qquad \text{Eq. (2.11)}$$

$$M_3 = \sqrt{\frac{2}{\gamma-1}\left(T_{2'}\left(\frac{1+\frac{\gamma-1}{2}\left(\frac{T_{2'}v_2}{T_2\sqrt{\gamma R T_{2'}}}\right)^2}{T_{2'}\left(\frac{P_1}{P_2}\right)}\right)-1\right)} \leq 1 \qquad \text{Eq. (2.12)}$$

As the exit pressure P_3 is known (=P_1), exit Mach number M_3 is calculated using Eq. (2.13)

$$M = \sqrt{\left(\left(\frac{P_{02'}}{P}\right)^{\frac{\gamma-1}{\gamma}}-1\right)\left(\frac{2}{\gamma-1}\right)} \qquad \text{Eq. (2.13)}$$

Also;

$$P_{02'} = P_{2'}\left(1+\frac{\gamma-1}{2}M_{2'}^2\right)^{\frac{\gamma}{\gamma-1}} \qquad \text{Eq. (2.14)}$$

$$T_{02'} = T_{2'}\left(1+\frac{\gamma-1}{2}M_{2'}^2\right) \qquad \text{Eq. (2.15)}$$

The sonic conditions are denoted by an asterisk. It can be shown that for an isentropic flow in a variable area duct

$$\left(\frac{A}{A^*}\right)^2 = \frac{1}{M^2}\left[\left(\frac{2}{\gamma+1}\right)\left(1+\frac{\gamma-1}{2}M^2\right)\right]^{\frac{\gamma+1}{\gamma-1}} \qquad \text{Eq. (2.16)}$$

It can also be shown that for an isentropic flow A^* is constant [6]. Using Eq. (2.16) at station 2′, A^* is obtained for region 2′ to 3. Similarly, A_3 is obtained from Eq. (2.16) using M_3. The Mach number and the pressure acting at all points is obtained from Eq. (2.16) and Eq. (2.13) respectively in region 2′ to 3. Net thrust provided by the engine is given by Eq. (2.6). Table 1 shows the sample calculation for obtaining performance parameters by following the above approach. All numerical modeling is carried out in Maple®18 [10].

A_2	1.26 m^2		A_2'	1.26 m^2
A_1	0.42 m^2		A_3	.92m^2
A_2/A_1	3		A_2'/A_3	1.36
P_1	101325 Pa		P_{01}	1.608334×10^5 Pa
T_1	288.15 K		P_{02}	1.475274×10^5 Pa
M_1	.84		A_3/A_1	2.21
P_2	1.567232×10^5 Pa		$F_{1\text{-}2}$	38108.64 N
T_2	326.39 K		$F_{2'\text{-}3}$	5751.34 N
M_2	0.19		F_{net}	32357.30 N
$M_{2'}$	0.45		$\dot{m}$	147.39 Kg/s
$P_{2'}$	1.282863×10^5 Pa		$F_{conventional}$	32354.83 N
T_2'	1200 K		$\eta_{p_{redefined}}$	15.34 %
M_3	0.75		$\eta_{p_{conventional}}$	57.55%

Table 1 *(Sample calculations for variable pressure combustion)*

2.1.5 Comparing thrust and efficiency with those obtained using conventional method

The formula for conventional propulsive efficiency of air-breathing engines is [11]

$$\eta_p = \frac{2}{1+\frac{c}{v}} \quad \text{Eq. (2.17)}$$

where c is the exhaust speed, and v is the speed of the aircraft. It lies in the range 0.2 - 0.9. In this case substituting the values of c (= M_3 a_3) and v (= M_∞ a_∞), η_p comes out to be 57.55%. The expression for thrust using Newton's laws is given by

$$\dot{m} = \rho_1 A_1 v_1 \quad \text{Eq. (2.18)}$$

$$F_{conventional} = \dot{m}(v_3 - v_1) \quad \text{Eq. (2.19)}$$

As shown in Table 1, the thrust values obtained by integrating the pressure forces and as given by Newton's laws ($F_{conventional}$) are equal, as expected. But the propulsive efficiency differs by a large margin which suggests that only a small fraction of the pressure forces are utilized to generate net thrust, and hence the engine model can be further improved for better utilization of pressure forces. This is because conventional efficiency ($\eta_{p_{conventional}}$) indicates the fraction of the net mechanical output that is converted into thrust power, whereas redefined propulsive efficiency ($\eta_{p_{redefined}}$) is an indicator of how efficiently an engine makes use of pressure profile. In a turbojet engine large fraction of thrust is negative thrust due to comparable exit area and inlet area, hence lower $\eta_{p_{redefined}}$.

2.1.6 Proof for the claim : $\mathbf{A_3 > A_1}$

For subsonic flow, the variation of A/A^* with M is shown in Fig. 3 which shows $A/A^* \propto 1/M$. It is obtained by plotting Eq. (2.16) using MATLAB. It can be easily proved that critical Area, A^*, always increases on addition of heat in a duct with subsonic inlet Mach number. Applying continuity equation, Eq.(2.18), on two critical cross sections, $\rho_1^* A_1^* a_1^* = \rho_2^* A_2^* a_2^*$ (cross section 1 is before addition of heat and cross section 2 is after addition of heat). From equation of state we have $\rho_1^*/\rho_2^* = (P_1^* T_1^*)/(P_2^* T_2^*)$ which on substitution in continuity equation gives, $A_2^*/A_1^* = (P_1^*\sqrt{T_2^*})/(P_2^*\sqrt{T_1^*})$. From isentropic relations we have, $P_1^*/P_2^* = P_{01}/P_{02}$ and hence $A_2^*/A_1^* = (P_{01}\sqrt{T_2^*})/(P_{02}\sqrt{T_1^*})$.

Temperature increases as a consequence of heat addition, that is $T_2^* > T_1^*$. For entropy to be positive, total pressure decreases after heat addition for subsonic flow [6,12] implying $P_{01} > P_{02}$. Therefore from the above arguments we have $A_2^* > A_1^*$. Yet again from isentropic relations, Eq. (2.13), Mach number is directly proportional to corresponding total pressure. So we can write $A/A^* \propto 1/P_0$. This is easily obtained by substituting M in terms of P_0 in Eq. (2.16) and then plotting using MATLAB, as shown in Fig. 4. Applying this relation to station 1 and station 3 gives $\frac{A_1/A_1^*}{A_3/A_2^*} = \frac{P_{02}}{P_{01}} \Rightarrow A_1/A_1^* < A_3/A_2^* \Rightarrow A_3 > A_1$.

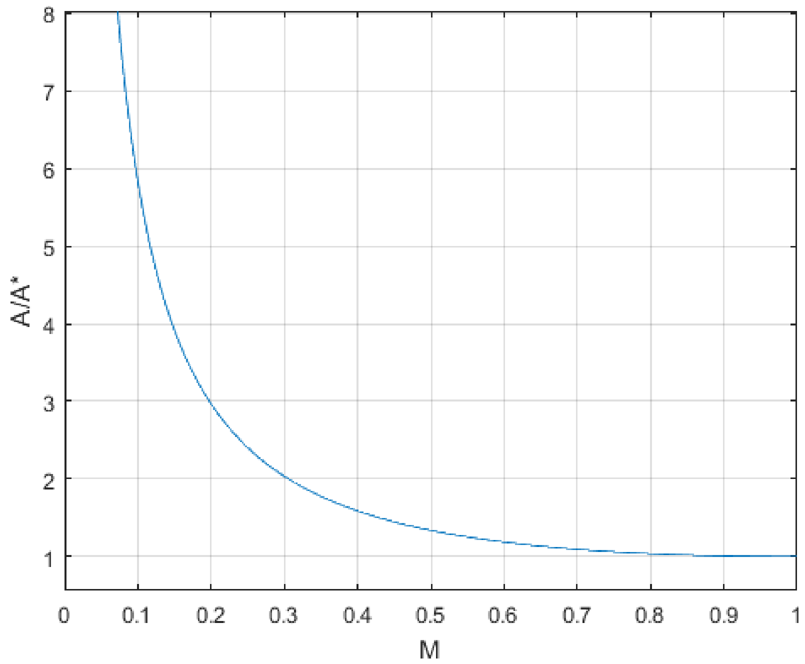

Fig.3 Variation of A/A^* with M for subsonic isentropic flow

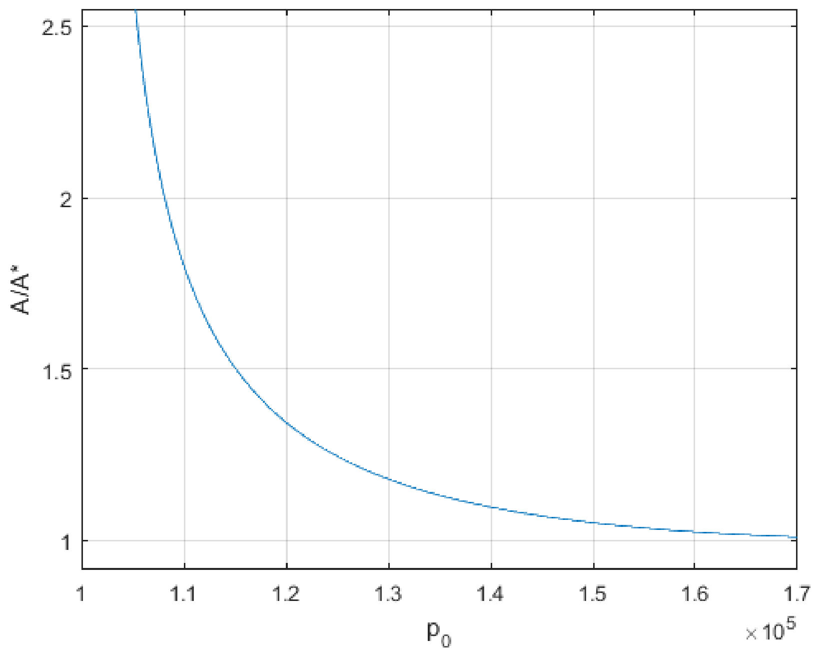

Fig.4 Variation of A/A^* with P_0 for subsonic isentropic flow

2.2 Constant pressure combustion in variable area duct

From the viewpoint of thermodynamic cycle efficiency, constant pressure combustion differs from variable pressure combustion and thus it is considered here. A variable area combustor that maintains a constant pressure is analyzed. Numerical modeling remains the same except that the flow parameters at 2′ will be different now. Conservation laws are applied to a small slab of the fluid in the region 2 - 2′ of Fig. 5 [8]. The law of conservation of mass gives Eq. (2.20)

$$\rho \mathrm{A} v = (\rho + \mathrm{d}\rho)(A + \mathrm{dA})(v + \mathrm{d}v) \Rightarrow \frac{\mathrm{d}v}{v} + \frac{\mathrm{dA}}{\mathrm{A}} + \frac{\mathrm{d}\rho}{\rho} = 0 \qquad \text{Eq. (2.20)}$$

The balance of the momentum in the direction of motion of fluid flow gives Eq. (2.21)

$$\dot{m}(v + dv) - \dot{m}v = PA - P(A + dA) + PdA \Rightarrow dv = 0 \qquad \text{Eq. (2.21)}$$

Eq. (2.21) signifies a constant velocity flow i.e. $v_2{}' = v_2$. Then from continuity equation, Eq.(2.18).

$$A_{2'}\rho_{2'} = A_2\rho_2 \Rightarrow A_{2'} = \frac{\rho_2 A_2 T_{2'} R}{P_2} \qquad \text{Eq. (2.22)}$$

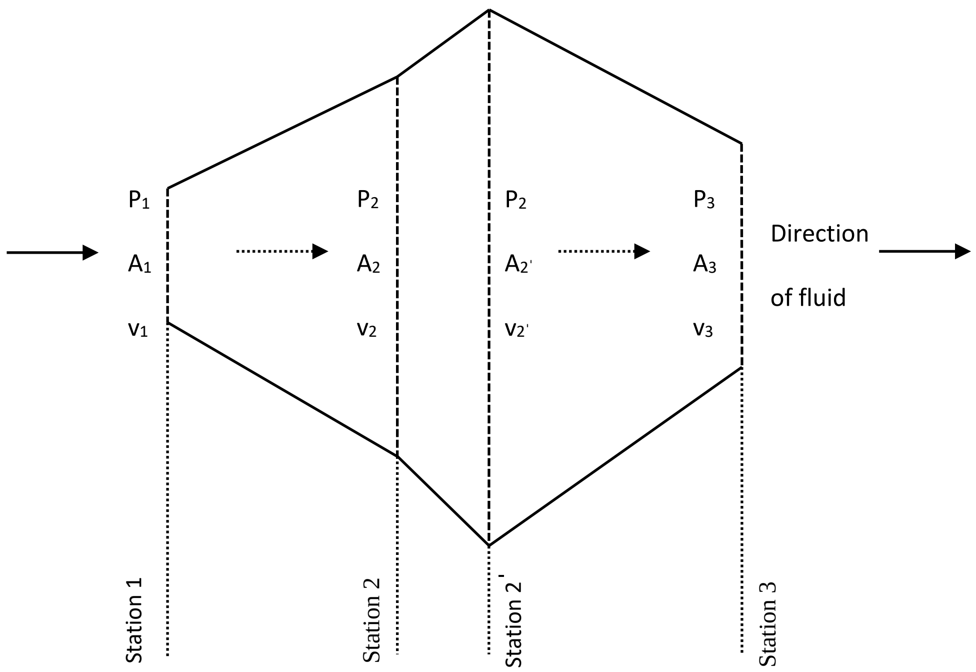

Fig.5 Theoretical model of turbojet engine for isobaric combustion

Since the combustor is modeled as a variable area duct, the outward normal of its surface subtends a positive angle (in I and IV quadrant) with the direction of the motion of aircraft. Hence the pressure forces acting on it contribute towards positive thrust. Table 2 shows the calculations carried out using the same initial conditions as in subsection *2.1.4.*

A_2	1.26 m^2
A_1	.42 m^2
A_2/A_1	3
P_1	101325 Pa
T_1	288.15 K
M_1	.84
P_2	1.567232×10^5 Pa
T_2	326.39 K
M_2	0.19
M_2'	0.1004
T_2'	1200 K
M_3	0.82
A_2'	4.64 m^2
A_3	.82 m^2

A_2'/A_2	3.67
A_2'/A_3	5.62
P_{01}	1.608334×10^5
P_{02}	1.578336×10^5 Pa
A_3/A_1	1.49
$F_{1\text{-}2}$	38108.64 N
$F_{2\text{-}2'}$	187245.956 N
$F_{2'\text{-}3}$	188469.022 N
F_{net}	36885.58 N
$\dot{m}$	147.39 Kg/s
$F_{conventional}$	36878.77 N
$\eta_{p_{redefined}}$	5.12 %
$\eta_{p_{conventional}}$	55.16%

Table 2 *(Sample calculations for constant pressure combustion)*

3. Comparing the Two Combustor Models

Conventionally thermal efficiency is defined as the ability of an engine to convert the thermal energy inherent in the fuel (which is unleashed in a chemical reaction) to a net kinetic energy gain of the working medium [7]

$$\eta_{th} = \frac{\dot{m}_a[(1+f)\frac{u_e^2}{2} - \frac{u^2}{2}]}{\dot{m}_f Q_R} \quad \text{Eq. (2.23)}$$

For $f << 1$

$$\eta_{th} = \frac{(\frac{u_e^2}{2} - \frac{u^2}{2})}{q} \quad \text{Eq. (2.24)}$$

Where $\dot{m}_a$ is the mass flow rate of incoming air, $\dot{m}_f$ is the mass flow rate of fuel injected, f is the ratio of the mass flow rate of air to the mass flow rate of fuel, Q_R is the heat of reaction of the fuel, $q = f\,Q_R$, u_e is the exhaust velocity and u is the inlet velocity. Basic thermodynamics claims that higher pressure ratio and higher operating temperature increase the efficiency of the Brayton cycle.

Table 3 shows a comparison between the two models. It can be interpreted from this table that isobaric combustion has a higher value of net thrust for similar conditions, because the normal to the surface of the isobaric combustor subtends an angle in I and IV quadrant with the direction of motion of the aircraft and hence contributes towards net positive thrust. The amount of heat addition required in variable pressure combustor is greater than that required for isobaric combustor. This is because of an increase in kinetic energy in variable pressure combustor which accounts for higher addition of heat for the same combustor exit temperature. Table 1 indicates a pressure decrease in variable pressure combustor ($P_2' < P_2$) due to expansion leading to an increase in exit area as compared to isobaric combustor (turbine inlet temperature and nozzle exit pressure is same for both cases), implying a lower value of negative thrust in the former. Due to the pressure drop in variable pressure combustor it does not require high negative gradient of flow track area in region 2′ to 3 for optimal expansion and hence have higher exit area (A_3). This results in lower value of negative thrust and higher redefined propulsive efficiency. That is, variable pressure combustor engines make better use of the pressure profile. For the same reason variable pressure combustor has lower value of exit Mach number (due to less amount of expansion).

	Variable pressure combustion	Isobaric combustion
$F_{positive}$	38108.64 N	225354.603 N
$F_{negatives}$	5751.34 N	188469.022 N
F_{net}	32357.30 N	36885.58 N
$\eta_{p_{redefined}}$	15.34 %	5.12 %
$\eta_{p_{conventional}}$	57.55%	55.16%
$\eta_{thermal}$	9.02%	11.22%
M_3	.75	.82
A_3/A_1	2.21	1.96
q	9.626227×10^5 J	9.159533×10^5 J

Table 3 *(Comparison between the two combustor models)*

4. Grid Convergence and Modeling Flow Track Area

In the model presented, the local pressure acting on the engine is just a function of the value of radius and does not depend on the length of the engine. As the dependence of the pressure forces on the length of the engine would make it a perpetual motion machine generating thrust without heat addition and only by varying the length of the region 1 to 2 and $2'$ to 3. The grid generated for the numerical modelling is one dimensional. The step size 'h' is constant. Having chosen the number of elements, say N, pose $h = \frac{b-a}{N}$ where b is the last element and a, the first element. Now, define $z_i = z_0 + ih$ with $z_0 = a$ and i = 0, 1, 2 … N. N is varied until the results obtained become independent of the length of the model. Then the solution is said to have converged for this value of N [13].

The procedure followed to calculate flow track area in region 1-2 is described here. Let $A_2/A_1 = k$ and length of the diverging region (1 to 2) be l_1 and z be the direction of motion of the aircraft. Then $r_2^2/r_1^2 = k$. Let $\alpha = 90 - \beta$. By simple geometric analysis of Fig. 1 $r_2^2/r_1^2 = k$ can be expanded as $(1-k)r_1^2 + 2l_1 tan\, \alpha_{1-2} + (l_1 tan\, \alpha_{1-2})^2 = 0$. This equation is solved to get r_1 and then

$$r_2 = r_1 + l_1 \tan(\alpha_{1-2}) \quad \text{Eq. (2.25)}$$

$$r = r_1 + z\tan(\alpha_{1-2}) \quad \text{Eq. (2.26)}$$

$$A = \pi r^2 \quad \text{Eq. (2.27)}$$

Similarly, flow track area in region 2′-3 is calculated as follows:-

$$r = r_{2'} - z\left(\frac{r_{2'} - r_3}{l_2}\right) \Rightarrow A = \pi r^2 \quad \text{Eq. (2.28)}$$

$$\tan \alpha_{2'-3} = \frac{r_{2'} - r_3}{l_2} \quad \text{Eq. (2.29)}$$

The procedure to calculate total pressure force acting on the engine is now explained. Let the total pressure force be denoted by F, then $F = \frac{F_{1-2}}{\sin \alpha_{1-2}} + \frac{F_{2'-3}}{\sin \alpha_{2'-3}}$. It could also be calculated by considering a frustum of area dA at location z from the inlet and integrating the pressure forces as :

$$F = \int (P - P_\infty) dA \quad \text{Eq. (2.30)}$$

Where

$$dA = \frac{2\pi r dr}{sin\alpha} \quad \text{Eq. (2.31)}$$

$$F = \int (P - P_\infty) \frac{2\pi r dr}{sin\alpha} \quad \text{Eq. (2.32)}$$

$$F = \int (P - P_\infty) \frac{2.\pi.r.dr}{sin\alpha_{1-2}} + \int (P - P_\infty) \frac{2.\pi.r.dr}{sin\alpha_{2'-3}} \quad \text{Eq. (2.33)}$$

5. Results and Discussions

1) Static pressure in region 1 to 2, as shown in Fig. 6 of theoretical jet engine increases (*variable pressure combustor*) . This happens due to an increase in flow track area of the subsonic flow and hence decrease in velocity (to maintain continuity) while there is an expansion occurring in

region 2′-3 due to a decrease in flow track area. This is also expected as diffusion takes place in the inlet and compressor of an airbreathing engine and expansion occurs in the turbine and nozzle as shown in Fig. 7.

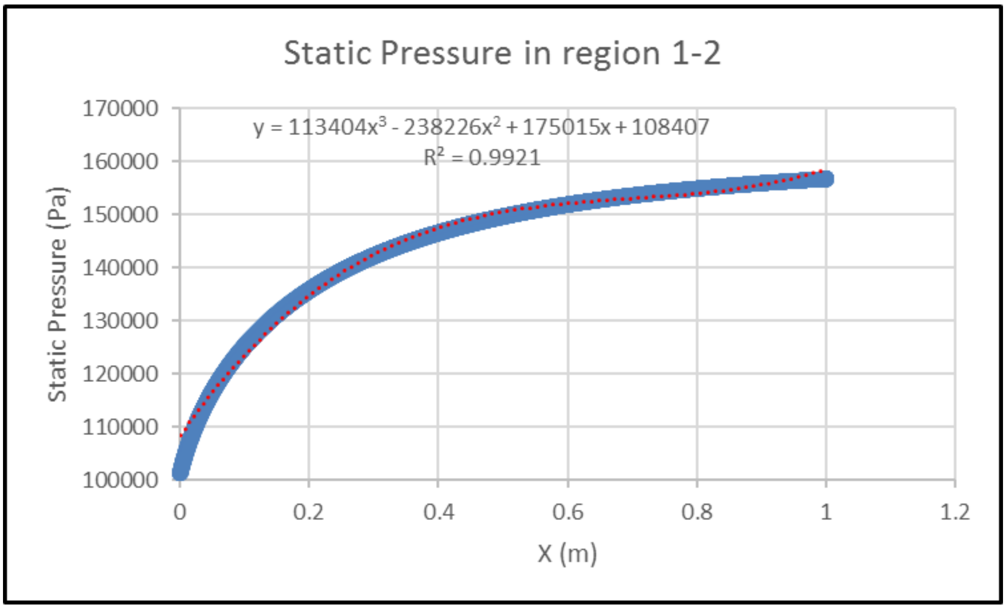

Fig.6 Variation of static pressure in region 1-2 (Variable pressure combustion) *(Plot obtained in Microsoft Excel 2016)*

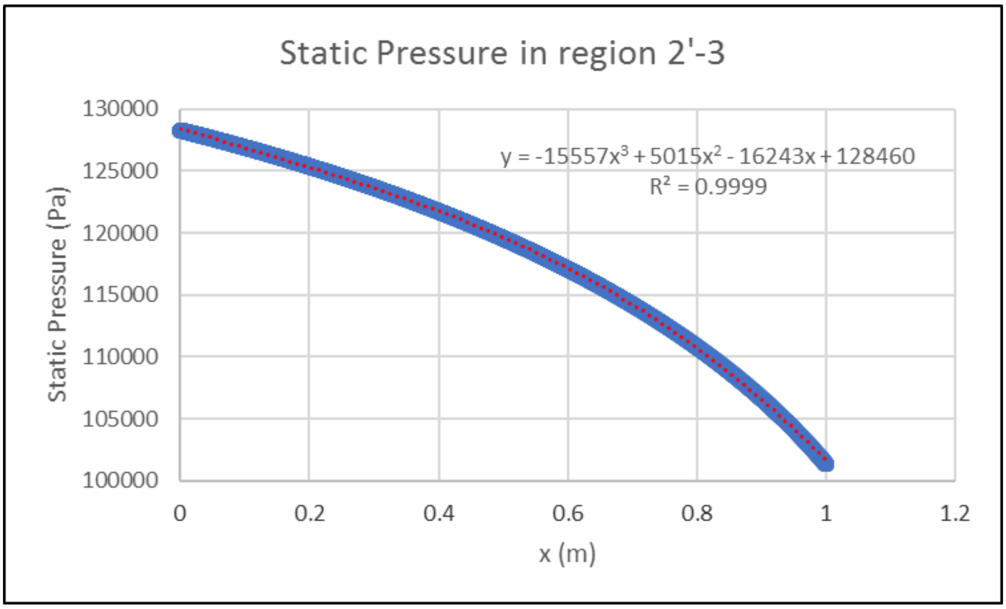

Fig.7 Variation of static pressure in region 2′ to 3 (Variable pressure combustion) *(Plot obtained in Microsoft Excel 2016)*

2) Due to heat addition in the combustion chamber total pressure will differ in two regions. It can be shown that addition of heat in constant area duct leads to increase in the entropy of the flow [12] implying that total pressure decreases after heat addition i.e. P_{01} (total pressure in region 1 to 2) > P_{02} (total pressure in region 2′ to 3).

3) The results obtained after numerical modeling indicate that thrust depends on the following parameters : inlet velocity (v_1), combustion temperature (T_2') and area ratio (A_2/A_1). Once the dimensions of the engine are fixed (i.e. A_2/A_1 is fixed) thrust increases with the combustion temperature (T_2') and inlet velocity v_1 as shown in the Fig. 8.

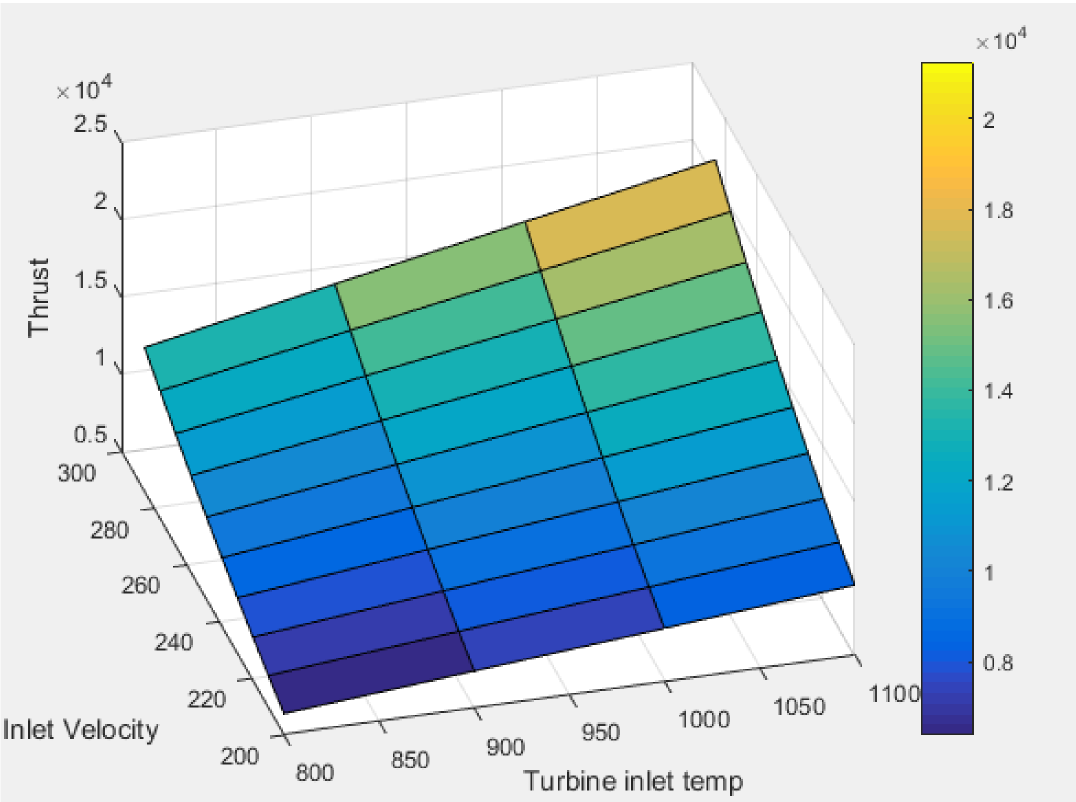

Fig.8 3D plot exhibiting the variation of net thrust with inlet velocity and combustion temperature (Variable pressure combustion) *(Plot obtained in MATLAB R2015b)*

4) The claim that the net positive thrust in a jet engine is generated due to an increase in exit area of engine ($A_3 > A_1$) is validated by numerical modelling. Simulations were carried out for different parameters (v_1, T_2', A_2/A_1) and resulted in $A_3 > A_1$ for net thrust to be positive. The exit area

value plays an important role while comparing isobaric combustor and variable pressure combustor as discussed below.

a. Isobaric combustion results in higher value of thrust due to contribution of positive thrust by the combustor. Heat addition is higher in variable pressure combustor due to increase in exit velocity of combustor with the same turbine inlet temperature and this increase in kinetic energy results in higher value of heat addition.

b. The variable pressure combustor has a higher value of $\eta_{p_{redefined}}$ as compared to isobaric combustor this is because of the difference in the exit area of the two models. Variable pressure combustor has larger exit area due to drop in pressure in the combustor and so does not require high negative gradient of flow track area in region $2'$ to 3. This decreases the contribution of negative thrust in variable pressure combustor and thereby higher redefined propulsive efficiency

5) The redefined propulsive efficiency increases with increase in turbine inlet temperature while it is approximately constant with the variation of the inlet velocity as shown in Fig. 9. This can be explained as, on increasing the operating temperature the work output from the engine increases and thereby increasing the net thrust.

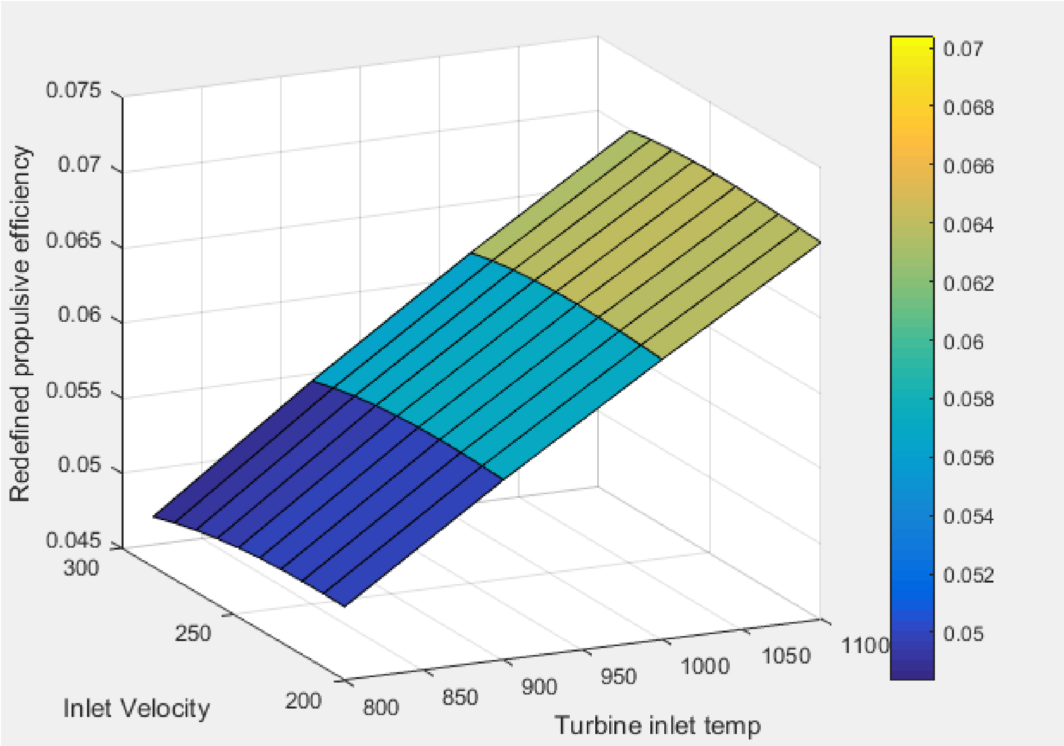

Fig.9 3 D plot exhibiting the variation of redefined propulsive efficiency with inlet velocity and turbine inlet temperature (Variable pressure combustion) *(Plot obtained in MATLAB R2015b)*

6) Redefined propulsive efficiency is much lower in magnitude as compared with conventional propulsive efficiency for both the cases. This is because conventional efficiency indicates the fraction of the net mechanical output that is converted into thrust power, whereas $\eta_{p_{redefined}}$ is an indicator of how efficiently an engine makes use of pressure profile. In a turbojet engine large fraction of thrust is negative thrust due to comparable exit area and inlet area, hence lower $\eta_{p_{redefined}}$. As the ratio of inlet and exit velocities is not too high $\eta_{p_{conventional}}$ has a higher value.

6. Conclusion

In this study a theoretical model was developed from first principles to formulate jet propulsion concepts and performance parameters, with the engine as center of interest and not the fluid exchanged as in the conventional approach. The engine thrust was defined as the surface integral of pressure forces exerted by the fluid on the surface of the jet engine. Similarly the propulsive efficiency was redefined as the efficiency with which the pressure forces are utilized for the generation of forward thrust. Two models of combustion were presented in details and comparison was carried out for different performance parameters of turbojet. This model can be extended to ramjet and scramjet to provide a theoretical basis to generate net positive thrust by developing an engine geometry that efficiently make use of the pressure profile.

7. References

[1] John Hiram Lewis III: Propulsive Efficiency from an Energy Utilization Standpoint. Journal of Aircraft Volume 13, No. 4. . April 1976

[2] Onder Turan. Anadolu University, School of Civil Aviation, 26470 Eskisehir, Turkey: Exergetic effects of some design parameters on the small turbojet engine for unmanned air vehicle applications. Energy. ELSEVIER. Volume 46. Issue 1. Pages 51-61. October 2012

[3] Yasin Şöhret & AliDinç & T. Hikmet Karakoç: Exergy analysis of a turbofan engine for an unmanned aerial vehicle during a surveillance mission. ELSEVIER. Volume 93. Part 1. Pages 716-729. December 2015

[4] Hakan Aydin & Onder Turan & T. Hikmet Karakoc & Adnan Midilli : Component–based exergetic measures of an experimental turboprop/turboshaft engine for propeller aircrafts and helicopters. International Journal of Exergy. Volume 11, Issue 3 (2012)

[5] Pedro Patrício and José M Tavares : Simple thermodynamics of jet engines. American Journal of Physics 78. July 2010

[6] Anderson J.D. 2002 : Modern Compressible Flow: With Historical Perspective. 3rd edition. McGraw-Hill Education

[7] Philip G. Hill and Carl R. Peterson : Mechanics and Thermodynamics of Propulsion. Addison-Wesley Publishing company

[8] Saeed Farokhi : Aircraft Propulsion . 2nd edition. John Wiley & Sons Ltd. Chapter 12.

[9] I. Martínez : Termodinámica básica y aplicada, Ed. Dossat. ISBN 84-237-0810-1 (1992)

[10] Maple user manual © Maplesoft, a division of Waterloo Maple Inc. 1996-2014. Version Maple18 and Purchase Ref. No.201302884/1 https://www.maplesoft.com/documentation_center/maple18/UserManual.pdf

[11] Loftin, LK, Jr. : Quest for performance : The evolution of modern aircraft. NASA SP-468. Appendix E. Retrieved 2006-04-22

[12] Patrick H. Oosthuizen and William Carscallen : Compressible Fluid Flow. McGraw-Hill companies, Inc(1997). 1st Edition

[13] Generation of 1D and 2D grids. In : Numerical Models for Differential Problems. MS&A, Volume 2. Springer, Milano

[14] Pearson, H. : Mixing of Exhaust and Bypass Flow in a Bypass Engine. Journal of the Royal Aeronautical Society. Volume.66. Pages 528-530. Aug.1962

[15] Rothrock, Addison M. : Turbojet Propulsion-System Research and the Resulting Effects on Airplane Performance. National Advisory Committee for Aeronautics; Washington, DC, United States. NACA-RM-54H23. Technical Report. Mar 17, 1955

[16] Seldner, K., Mihaloew, J. R., Blaha, R. J. : Generalized simulation technique for turbojet engine system analysis. NASA Lewis Research Center, Cleveland, OH, United States. NASA-TN-D-6610, E-5998. Technical Report. Feb 01, 1972